CHEMISTRY & SUSTAINABILITY

CHEMSUSCHEM

ENERGY & MATERIALS

Accepted Article

Title: Light-Harvesting Organic Nanocrystals Capable of Photon Upconversion

Authors: Li Li, Yi Zeng, Tianjun Yu, Jinping Chen, Guoqiang Yang, and Yi Li

To be cited as: *ChemSusChem* 10.1002/cssc.201701389

Link to VoR: http://dx.doi.org/10.1002/cssc.201701389

A Journal of

ChemPubSoc Europe

WILEY-VCH

www.chemsuschem.org

10.1002/cssc.201701389

WILEY-VCH

Light-Harvesting Organic Nanocrystals Capable of Photon Upconversion

Li Li, [a] Yi Zeng,*[a] Tianjun Yu,[a] Jinping Chen,[a] Guoqiang Yang,[b] and Yi Li*[a]

Abstract: Harvesting and converting low energy photons to higher ones through upconversion have great potential in solar energy conversion. Herein, we demonstrate a light-harvesting nanocrystal assembled by 9,10-distyrylanthracene and palladium(II) *meso*-tetraphenyltetrabenzoporphyrin as the acceptor and the sensitizer, respectively, in which red-to-green upconversion is achieved under incoherent excitation of low power density and the upconversion quantum yield of 0.29 ± 0.02% is obtained upon excitation with 640 nm laser of 120 mW cm^{-2}. The well-organized packing of acceptor molecules with aggregation-induced emission in the nanocrystals dramatically reduces the nonradiative decay of the excited acceptor, benefits the TTA upconversion and guides out the consequent upconverted emission. This work provides a straightforward strategy to develop light-harvesting nanocrystals based on TTA upconversion, which is attractive for energy conversion and photonic applications.

Introduction

Solar energy has been considered as one of the most promising renewable energy resources. Collection and conversion of solar energy by mimicking photosynthesis is one major area of endeavor in sustainable chemistry research, because photosynthesis is the most elegant way to utilize solar energy and has powdered live beings on earth for billions of years. The photosynthesis is initiated with light absorption by light-harvesting components, followed by series energy migration and transfer and finally funneling into reaction centers.[1] The unique function has stimulated chemists to created artificial ways to harvest solar energy and a large number of artificial light-harvesting systems based on molecular and supramolecular complexes have been developed.[2-4] In order to meet the increasing demands of solar energy conversion, it is desirable to harvest as much energy from sunlight as possible, especially those low energy photons that do not meet bandgaps or absorption thresholds of conventional light-harvesting materials. A potential way to raise the efficiency of solar energy conversion is employing photon upconversion, by which low energy photons convert to higher energy photons allowing them to be used by conventional solar converters.[5-8]

Photon upconversion has great potentials in solar energy conversion and photonic techniques because it generates higher-energy photons through absorbing lower energy photons by excitation with low-power and noncoherent light source. There are two distinct ways to achieve photon upconversion, lanthanide ions-based upconversion and triplet-triplet annihilation (TTA) upconversion.[9] Photon upconversion based on TTA involves a two-component system consisting of sensitizer and acceptor (or called annihilator).[5, 10, 11] The sensitizers capture lower-energy photons and undergo intersystem crossing (ISC) forming the triplet excited sensitizers, which give birth to triplet excited acceptors through triplet-triplet energy transfer (TTET). Two triplet acceptors encounter within their lifetime and the TTA process takes place, generating a singlet excited acceptor and the consequent upconverted fluorescence. TTA upconversion shows advantages over lanthanide upconversion systems, such as potentially higher upconversion efficiency, lower power density of excitation, and broad spectral tunability. However, unlike the lanthanide upconversion systems which have been widely produced as lanthanide ion-doped nanomaterials with controlled size, shape, and function, it is still a tough issue to achieve efficient TTA upconversion of solid systems due to the requirement of diffusion and proximity of photoactive components to guarantee serial Dexter-type energy transfers during conventional TTA upconversion. After continuous efforts in the past decade, diversified strategies have been made in solidification or immobilization of TTA upconversion by introducing inner matrixes, such as polymeric backbone, gels, capsules and vacuum deposition.[12-20] Those blending and encapsulation approaches have made a step forward into a solid or quasi-solid state, thus advancing the application of TTA upconversion in practical devices. Nevertheless, it is still challenging to achieve crystalline TTA upconversion systems, and obstacle factors including microphase segregation, limited molecular diffusion and self-quenching of excited chromophores in aggregate states still need to be addressed for improving upconversion performance.[7,21,22]

Sensitized TTA upconversion in organic crystals and the triplet exciton fusion therein as well as the magnetic field effects have been studied theoretically and experimentally decades ago.[23-25] More recently, metal-organic frameworks (MOFs) architectures with well-aligned chromophores and effective exciton diffusion have been applied to efficient TTA upconversion under low power excitation,[26] however, there

[a] L. Li, Dr Y. Zeng, T. J. Yu, J. P. Chen, Prof. Dr. Y. Li
Key Laboratory of Photochemical Conversion and Optoelectronic Materials, Technical Institute of Physics and Chemistry
University of Chinese Academy of Sciences
Chinese Academy of Sciences
Beijing 100190, China
E-mail: zengyi@mail.ipc.ac.cn; yili@mail.ipc.ac.cn
[b] Prof. Dr. G. Q. Yang
Beijing National Laboratory for Molecular Sciences (BNLMS), Key Laboratory of Photochemistry, Institute of Chemistry
University of Chinese Academy of Sciences
Chinese Academy of Sciences
Beijing 100190, China

Supporting information for this article is given via a link at the end of the document.

are still limited successes in crystals or nanocrystals for efficient TTA upconversion.[26-28] Organic nanocrystals composed of small molecules with special photophysical or optoelectronic properties have attracted great interest because of their function versatility in fundamental studies and practical applications including bioimaging, nanophotonic and optoelectronic devices.[29-32] By harnessing the flexibility of organic molecule tailoring and assembling, organic nanocrystals capable of efficient photon upconversion via TTA show great potential in solar energy conversion, although the design and preparation is still challenging.

Here, we present a straightforward approach for TTA upconversion nanocrystals based on acceptors nanocrystals doping with sensitizer. The upconversion chromophore pair consists of a porphyrin-type sensitizer, palladium(II) meso-tetraphenyltetrabenzoporphyrin (PdTPTBP), and an acceptor, 9,10-distyrylanthracene (DSA), with aggregation-induced emission (AIE) property. AIE chromophores, different from traditional dyes with aggregation caused quenching, are non-emissive or weakly emissive in molecularly dissolved solution but highly emissive in aggregate or solid-state mainly due to the restriction of intramolecular motions, which restrains nonradiative decays and consequently benefits the aggregate or solid-state emission.[33, 34] The doped nanocrystal is fabricated through a single-step solution-based crystallization assisted by sodium dodecyl sulfate (SDS). It is found that the nanocrystals of DSA acceptor doped with PdTPTBP effectively upconvert red photons to green ones. This study provides a versatile strategy to develop upconversion nanocrystals based on TTA for energy and photonic applications.

Results and Discussion

PdTPTBP and DSA (Figure 1a) are prepared according to previous reports and the structures are characterized by NMR and MS.[35-38] The acceptor DSA and its analogues exhibit typical AIE behaviors with high fluorescence quantum yield at solid-state and have been used as aggregate or solid-state emitters for bioimaging, sensing, and mechanochromism applications.[39-41] DSA molecules in crystals adopt a slipped-cofacial packing structure due to the non-coplanar conformation of the styryl substituent and anthracene core, which endows DSA crystals with high emission quantum yield and waveguide function, making them as promising photonic materials.[39] The absorption and emission spectra of PdTPTBP and DSA are shown in Figure 1b. PdTPTBP shows strong absorption in the region of 400–460 and 600–650 nm with peaks at 441 (Soret-band) and 628 nm (Q-band), respectively. It emits phosphorescence with maximum at about 800 nm at room temperature and its reported ISC efficiency is near unity.[36] PdTPTBP has been applied as the sensitizers in various TTA upconversion systems and the photophysical process therein have also been investigated in depth.[42-45] The absorption of DSA lies below 500 nm with smaller extinction coefficient compared to that of PdTPTBP. The crystalline DSA displays narrow emission around 514 nm mostly located at the transmission window between the Soret- and Q-bands of PdTPTBP, partially alleviating the energy transfer from the excited singlet DSA to PdTPTBP.

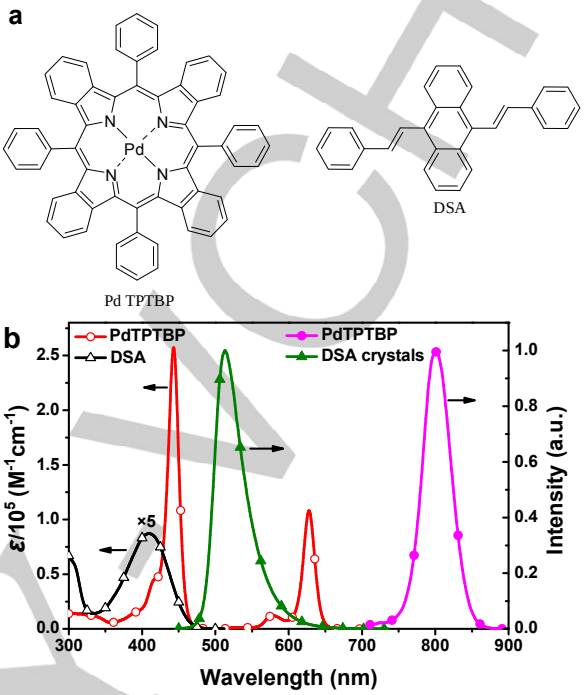

Figure 1. (a) Structures of the sensitizer PdTPTBP and the acceptor DSA. (b) Absorption spectra of PdTPTBP and DSA and normalized emission spectra of PdTPTBP in deaerated toluene and DSA crystals. λ = 414 nm.

The phosphorescence of PdTPTBP can be readily quenched by DSA. The free-energy change (ΔG) involved in an electron transfer process from the triplet PdTPTBP to DSA is determined to be positive (+1.61 eV) according to Rehm-Weller equation, indicating that the electron transfer process is endothermic and thermodynamically unfavorable. It is proposed that triplet-triplet energy transfer from PdTPTBP to DSA accounts for the phosphorescence quenching upon addition of DSA into the PdTPTBP solution. The efficiency of triplet-triplet energy transfer is estimated to be near unity in toluene with a sensitizer/acceptor ratio of 1/800, as verified by the steady-state and time-resolved phosphorescence quenching (Figure S1 in Supporting Information). However, no upconverted emission is detected in solution-based systems upon selective excitation of PdTPTBP using 640 nm laser of up to 120 mW cm^{-2}. It can be rationalized by the severe nonradiative decay caused by intramolecular rotations of DSA in solution (the fluorescence quantum yield of DSA in toluene is determined to be 1.1%), which deactivate either triplet excited DSA or the possible singlet DSA formed from TTA.

To obtain nanocrystals for TTA upconversion, we apply an approach employing solution-based self-assembly of organic compounds which is a mild and facile technique to prepare organic nanocrystals with various morphologies and doping compositions. In this work, the TTA upconversion nanocrystals

are prepared by SDS assisted assembly of PdTPTBP and DSA in aqueous solution. A THF solution of PdTPTBP (5 μM) and DSA (4 mM) is rapidly injected into a SDS aqueous solution (10 mM), which is stirred vigorously for 10 mins and then stabilized for 24 hours. The obtained colloidal solution is subjected to centrifugation giving the doped self-assembly sample as light yellow solids. Scanning electron microscopy (SEM) measurement demonstrates that these compounds self-assembly into nanorods of about 150-200 nm in average width and 1–3 μm in length, which possess rectangular cross-section and good morphological purity (Figure 2a). Transmission electron microscopy and selected area electron diffraction (SAED) pattern (Figure 2b) reveal that the doped nanorods possess uniform crystal structures growing along the [001] direction. X-ray diffraction (XRD) patterns were also recorded to further investigate the crystal structure of these nanorods (Figure 2c). The evident diffraction peaks from the doped nanorods confirm the highly crystalline structure of the nanorods and the similar patterns to that of the DSA single crystals, verifying that the doping of such amount of the photosensitizer has little effect on the crystalline structure of DSA in nanorods.

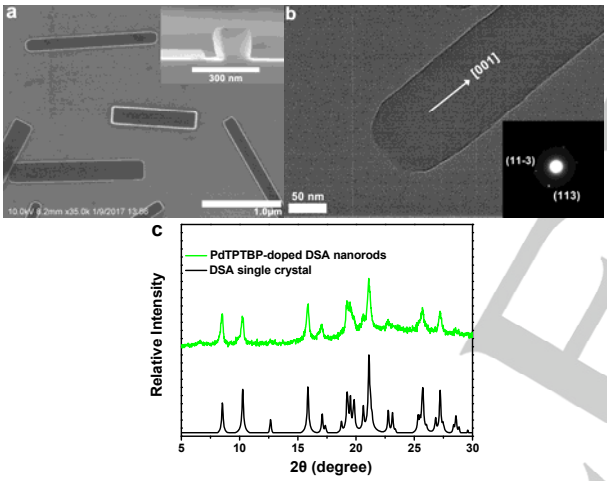

Figure 2. (a) SEM image of PdTPTBP-doped DSA nanorods. Inset shows the cross section of a nanorod. (b) TEM image and SAD pattern of DSA. (c) XRD patterns of DSA single crystal (reference no. CCDC 688692) and the doped nanorods from bottom to top.

The nanorods show clear green emission with a fluorescence characteristic of the DSA crystal with a maximum at 514 nm upon excitation with 640 nm laser. The observation of upconverted emission implies the occurrence of TTA upconversion in the nanorods, which is indicated further by the control experiments that neat DSA or PdTPTBP crystals show no detectable luminescence with wavelength shorter than the excitation light under the same experimental conditions. Apparent upconversion emission from the nanocrystals under air can also be observed as the impeded diffusion of oxygen into the crystals, however, the upconversion intensity decreases gradually upon irradiation which may be due to the oxidation of the nanocrystals by singlet oxygen generated by the triplet chromophores. To characterize the TTA upconversion property, the doped nanorods from co-assembly of PdTPTBP and DSA is sandwiched between two quartz coverslips in a glove box filled with argon (O_2 concentration < 0.1 ppm) and sealed by epoxy adhesive. Upconversion luminescence imaging of the nanorods was performed on a confocal microscope with continuous wave (CW) laser of 640 nm as the excitation source. All of the nanorods show evident upconversion emission, indicating that sensitizers are well distributed in DSA-based nanorods (Figure S5). Furthermore, the upconverted emission spectra were collected by using an integrating sphere coupled to a spectrometer with a liquid-nitrogen cooled CCD upon excitation with different intensities of 640 nm laser and the double logarithmic plots of the upconversion emission intensity as a function of the incident light power are presented in Figure 3a. The intensity of upconverted green emission shows dependence on the incident power from quadratic to linear as increasing the excitation laser power, which strengthens that the upconverted emission originates from the TTA upconversion.[46,47] Two linear regions fitted to the slopes of 1.9 and 1.2 have been demonstrated, which correspond to the low- and high-power density regimes, respectively. The threshold excitation intensity I_{th}, defined as the slope transition point,[47] is evaluated to be 35.9 mW cm^{-2} for 640 nm excitation light. After I_{th} the TTA process of excited triplet acceptors surpasses the spontaneous decay and the upconversion emission intensity starts to be linearly dependent to the incident power.

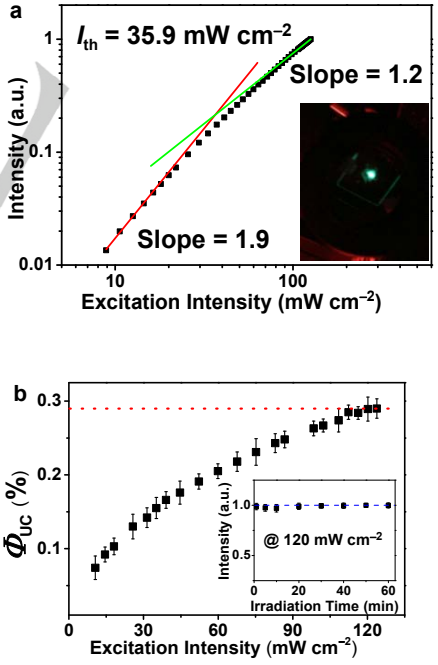

Figure 3. (a) Upconversion emission intensity of the doped nanorods changes with the excitation intensity of 640 nm laser. The two linear fitting with slops of 1.9 (red) and 1.2 (green) are presented and the extrapolated intersection of the two fitting lines indicates the threshold excitation intensity (I_{th}). Inset shows a photo of the nanorods sealed between coverslips taken behind a 500–520 nm bandpass filter under irradiation with a 640 nm CW laser. (b) Upconversion quantum yields of the doped nanorods as a function of the excitation intensity.

Inset shows time-dependent upconversion emission intensity of the nanorods under continuous irradiation with 640 nm laser at 120 mW cm^{-2}.

The upconversion efficiency is described by upconversion quantum yield (Φ_{UC}) which is defined as the ratio of emitted upconversion photons to absorbed photons with a theoretical maximum of 50%. The absolute upconversion quantum yield of the nanorods is quantified by using an integrating sphere coupled to a spectrometer with a liquid-nitrogen cooled CCD and following the reported method in the literature.[48] Φ_{UC} of the nanorods are measured at various excitation intensities and an average Φ_{UC} of (0.29 ± 0.02)% is obtained at the incident laser intensity of 120 mW cm^{-2}. The upconversion emission in the nanorods is likely attributed to the blockage of nonradiative relaxation of the excited DSA state caused by the restraint of free intramolecular torsional motions in solid-state. Adjacent packing of the acceptor molecules in the crystalline material makes the triplet exciton diffusion and thus the subsequent TTA upconversion possible in molecular diffusion-free environment. The waveguide property may help to guide out the upconverted emission within the nanocrystals[39] Furthermore, the TTA upconversion nanorods show steady upconversion emission under continuous irradiation at 120 mW cm^{-2} for 60 minutes (Figure 3b), indicating the good photostability. The air-stability of the epoxy-sealed sample was also examined and the result showed that the upconversion efficiency of the sample can be maintained at ambient conditions for more than 28 days indicating of the good gas proofness of the epoxy-sealed device (Figure S3 in Supporting Information).

The photophysical processes within the upconversion nanomaterial are further investigated by steady-state and time-resolved spectroscopy. The phosphorescence of PdTPTBP nanoaggregates dispersed in SDS (~ 110 nm diameter) shows a mono-exponential decay with a lifetime of τ_0 = 367 μs, while in the PdTPTBP-doped DSA nanorods, the phosphorescence of PdTPTBP decays rapidly and the dynamic trace almost overlaps with the instrument response function (IRF, ~9 μs), which is consistent with the observation of phosphorescence quenching of PdTPTBP by DSA in toluene solution. A TTET efficiency (Φ_{TTET}) of about 97% was estimated by considering these two lifetimes. The phosphorescence quantum yields of PdTPTBP nanoaggregates dispersed in SDS and PdTPTBP doped DSA nanomaterials are measured to be 2.6% and 0.06%, respectively, providing the same TTET efficiency as those estimated by phosphorescence lifetime measurements. The fluorescence quantum yield (Φ_F) of neat DSA crystals is measured to be 39%. Thus, the triplet-triplet annihilation efficiency Φ_{TTA} of about 0.76% is obtained for the upconversion nanocrystal according to the relationship $\Phi_{UC} = \Phi_{ISC}\Phi_{TTET}\Phi_{TTA}\Phi_F$. The time-resolved upconversion emission of the doped nanocrystal was also measured. The fluorescence lifetime of the acceptor extends into the microsecond region as depicted in Figure 4, demonstrating a delayed fluorescence feature and strengthening the occurrence of the TTA upconversion. The generation of upconversion emission is prompt and no rising dynamics is observed under the experiment condition. No transient absorption of the acceptor could be detected in transient absorption measurements. To estimate the triplet lifetime of the acceptor (τ_T), which affects the TTA upconversion efficiency, we use the following approximation function. When the triplet-triplet annihilation rate is much smaller or negligible compared with the spontaneous decay of the acceptor triplet in the longer time region, there is an approximation $I_{UC}(t) \propto \exp(-t/\tau_{UC}) = \exp(-2t/\tau_T)$, where τ_{UC} is the upconversion emission lifetime and τ_T is the lifetime of the acceptor triplet[27, 49]. Based on this relationship, a τ_T value of 5.2 μs is estimated for the triplet DSA by fitting the tail of the kinetic trace of the upconverted emission. The relatively short lifetime of the acceptor triplet limits the triplet diffusion distance and encounter probability. The triplet lifetime of acceptors needs to be extended to improve the upconversion efficiency and may be improved by new molecular design or introducing rigid framework confinement.[50]

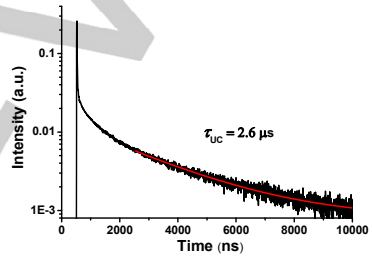

Figure 4. Kinetic profile of the delayed fluorescence observed in the nanorods excited with 635 nm pulse laser (~7 ns pulse from OPO laser). The solid red line indicates the exponential fit of the tail of decay trace.

Conclusion

In summary, a promising approach for light-harvesting nanomaterials capable of photon upconversion based on acceptors nanocrystals doped with sensitizers has been demonstrated. An acceptor with aggregation-induced emission is adopted in combination with a porphyrin-type sensitizer to construct the sensitizer-acceptor pair of TTA upconversion system. The doped nanocrystal is fabricated through a single-step solution-based crystallization assisted by surfactant. The doped-nanocrystals upconvert red excitation photons into green emission with an upconversion quantum yield of about 0.29% on account of the well-defined alignment of AIE acceptor molecules in the nanocrystals which dramatically reduce the nonradiative decay of the excited acceptor and benefit the consequent TTA upconversion. The fluorescence quantum yield of DSA crystals is about 0.4 and there are still plenty rooms to improve the TTA upconversion by developing AIE acceptors with higher fluorescence quantum yields, since a lot of AIE compounds show near 100% fluorescence quantum yields. In addition, it is a potential way to incorporate classic chromophore units with high TTA efficiency into AIE acceptors, and enhance the triplet diffusion and TTA process. Rigid frameworks or environmental effects can be introduced into the AIE systems to extend the triplet lifetime which is also a feasible way to improve the TTA

upconversion. This study provides a potential strategy to develop light-harvesting nanocrystals based on TTA upconversion, which is attractive for solar energy conversion and photonic applications by harnessing the modification and tunability of morphology, size, surface functionality from organic nanocrystals.

Experimental Section

Materials

Reagents were purchased from Aldrich or Innochem or J&K chemical and were used without further purification, unless otherwise noted. Palladium(II) tetraphenyltetrabenzoporphyrin (PdTPTBP)[32] and 9,10-distyrylanthracene (DSA)[33] were prepared according to literature reports.

PdTPTBP is obtained as dark green powder with a total yield of 3%. ^{1}H NMR (400 MHz, DMSO-*d6*) δ 8.25 (d, *J* = 7.1 Hz, 8H), 8.03 (d, *J* = 7.4 Hz, 4H), 7.96 (t, *J* = 7.5 Hz, 8H), 7.31-7.29 (m, 8H), 7.07-7.04 (m, 8H). MS(MALDI/TOF) calcd. m/z for M^+ 918.2, found 918.2.

DSA is prepared by Heck coupling of styrene and 9,10-dibromoanthracene and obtained as yellow solid (yield 55%). mp: 276.7–278.4 ºC. ^{1}H NMR (400 MHz, $CDCl_3$) δ 8.41 (dd, *J* = 6.7, 3.1 Hz, 8H), 7.94 (d, *J* = 16.5 Hz, 2H), 7.70 (d, *J* = 7.4 Hz, 4H), 7.48 (dd, *J* = 10.2, 5.1 Hz, 8H), 7.37 (t, *J* = 7.3 Hz, 2H), 6.95 (m, *J* = 16.5 Hz, 2H). ^{13}C NMR (101 MHz, $CDCl_3$) δ 137.50, 137.35, 132.72, 129.61, 128.86, 128.05, 126.62, 126.48, 125.26, 125.21. MS(EI-TOF) calcd. m/z for M^+ 382.1722, found 382.1723.

Preparation of samples for upconversion

Quartz coverslips (φ 25 mm × 25 mm × 0.2 mm) were washed by continuous sonication in detergent solution for 30 mins, cleaned by deionized water, ethanol and dichloromethane, and then dried by a stream of compressed nitrogen.

The PdTPTBP-doped DSA nanocrystals were prepared by a solution-based nanocrystallization process. A 4mL THF solution containing PdTPTBP (0.005 mM) and DSA (4 mM) was rapidly injected into 25 mL sodium dodecyl sulfate (SDS, 10 mM) aqueous solution under vigorous stirring. After being stirred for 10 mins and standing for 24h at 25 ºC, the obtained colloidal solution was subjected to centrifugation at 3,000 rpm for 3 mins to remove large precipitates. The doped nanocrystals were collected by centrifugation at 9,000 rpm for 10 mins. The nanocrystals were dried under vacuum and sealed between two quartz coverslips using two-component epoxy adhesive (Ergo 7300) in a glovebox charged with argon (O_2 concentration < 0.1 ppm).

Instrumentation

^{1}H NMR spectra were recorded with a Bruker Avance P-400 (400 MHz) spectrometer with tetramethylsilane as an internal standard. Scanning electron microscopy (SEM) images were obtained using the HITACHI S-4800 with nanocrystals casted on silicon substrate. TEM images were performed using JEM-2100 with samples placed on holey copper grids. X-ray powder diffraction (XRD) patterns were measured at a scanning rate of 5 deg/min in the 2θ range from 5° to 50° with a Bruker D8 Focus X-ray diffractometer equipped with Cu Kα radiation (λ = 1.54050 Å). Confocal upconversion imaging of nanorods was performed on a confocal microscope (Nikon-C2-SIM) equipped with 500–550 nm filter and a CW laser of 640 nm.

Absorption and emission spectra were measured by using a Shimadzu UV-2550PC spectrometer and a Hitachi F-4600 spectrometer, respectively. The phosphorescence lifetimes of PdTPTBP were recorded on an Edinburgh FLS920 spectrometer excited with a μs flash lamp (~2 μs FWHM). The decay dynamics of the upconverted fluorescence was monitored on an Edinburgh LP920 spectrometer equipped with nanosecond pulse laser (~7 ns FWHM) provided by the combination of Nd:YAG laser and OPO.

Upconversion emission spectra and emission quantum yields were recorded in an integrating sphere (Labsphere) combining to a Princeton Instrument Acton SP2500 spectrograph and a SPEC-10 liquid nitrogen-cooled CCD. The upconversion quantum yields of nanocrystals and the fluorescence quantum yield of DSA crystals were measured by excitation with 640 and 405 nm CW lasers (PicoQuant LDH-D-C-series), respectively, following the method reported in literature.[19]

The free-energy change (ΔG) of a electron transfer process was calculated according to Rehm-Weller equation:

$$\Delta G = e[E_{OX}\text{-}E_{RED}] - E_{0,0} - \frac{e^2}{4\pi\varepsilon_0\varepsilon_S R_{CC}} - \frac{e^2}{8\pi}\left(\frac{1}{R_D}+\frac{1}{R_A}\right)\left(\frac{1}{\varepsilon_{REF}}-\frac{1}{\varepsilon_S}\right)$$

E_{OX} and E_{RED} are the oxidation potential of electron donor (PdTPTBP) and the reduction potential of electron acceptor (DSA), respectively, which are 0.61 V and -2.07 V in THF with reference to Fc/Fc^+. $E_{0,0}$ represents the triplet excited state energy of PdTPTBP, which is 1.56 eV. ε_S = static dielectric constant of the solvent, R_D is the radius of the donor, R_A is the radius of the electron acceptor, ε_{REF} is the static dielectric constant of the solvent used for the electrochemical studies(7.58 for THF), ε_0 permittivity of free space. The solvents used in the calculation of free energy of the electron transfer is toluene (ε_S = 2.38). The distance between the donor and the acceptor (r_{cc}) is about 55 Å. To estimate the Born correction to the solvation energy, we set R_D and R_A equal to 8.3 and 5.9 Å, respectively, by assuming that both donor and acceptor are spherical. The value of ΔG in toluene is calculated to be +1.61 eV.

Acknowledgements

Financial support from the 973 program (2013CB834703 and 2013CB834505), the National Natural Science Foundation of China (Nos. 21233011, 21673264, 21573266, 21472201 and 21672226), and the Strategic Priority Research Program (XDB17030300) and Youth Innovation Promotion Association (2017032) of Chinese Academy of Sciences is gratefully acknowledged.

Keywords: light harvesting • photochemistry • nanoparticles • photon upconversion • aggregation

[1] T. Mirkovic, E. E. Ostroumov, J. M. Anna, R. van Grondelle, Govindjee, G. D. Scholes, *Chem. Rev.* **2017**, *117*, 249.
[2] V. Balzani, A. Credi, M. Venturi, *ChemSusChem* **2008**, *1*, 26.
[3] X. H. Zhang, Y. Zeng, T. J. Yu, J. P. Chen, G. Q. Yang, Y. Li, *J Phys Chem Lett* **2014**, *5*, 2340.
[4] S. Kundu, A. Patra, *Chem. Rev.* **2017**, *117*, 712.
[5] T. N. Singh-Rachford, F. N. Castellano, *Coord. Chem. Rev.* **2010**, *254*, 2560.
[6] P. Ceroni, *Chem-Eur J* **2011**, *17*, 9560.
[7] T. F. Schulze, T. W. Schmidt, *Energy Environ. Sci.* **2015**, *8*, 103.
[8] Y. Zeng, J. Chen, T. Yu, G. Yang, Y. Li, *ACS Energy Letters* **2017**, *2*, 357.
[9] J. Zhou, Q. Liu, W. Feng, Y. Sun, F. Y. Li, *Chem. Rev.* **2015**, *115*, 395.
[10] J. Z. Zhao, S. M. Ji, H. M. Guo, *Rsc Adv.* **2011**, *1*, 937.
[11] T. W. Schmidt, F. N. Castellano, *J. Phys. Chem. Lett.* **2014**, *5*, 4062.
[12] P. E. Keivanidis, S. Baluschev, T. Miteva, G. Nelles, U. Scherf, A. Yasuda, G. Wegner, *Adv. Mater.* **2003**, *15*, 2095.
[13] R. R. Islangulov, J. Lott, C. Weder, F. N. Castellano, *J. Am. Chem. Soc.* **2007**, *129*, 12652.

[14] C. Zhang, J. Y. Zheng, Y. S. Zhao, J. N. Yao, *Chem. Commun.* **2010**, *46*, 4959.
[15] Y. C. Simon, C. Weder, *J. Mater. Chem.* **2012**, *22*, 20817.
[16] J. H. Kim, F. Deng, F. N. Castellano, J. H. Kim, *Chem. Mater.* **2012**, *24*, 2250.
[17] A. Monguzzi, F. Bianchi, A. Bianchi, M. Mauri, R. Simonutti, R. Ruffo, R. Tubino, F. Meinardi, *Advanced Energy Materials* **2013**, *3*, 680.
[18] P. F. Duan, N. Yanai, H. Nagatomi, N. Kimizuka, *J. Am. Chem. Soc.* **2015**, *137*, 1887.
[19] M. F. Wu, D. N. Congreve, M. W. B. Wilson, J. Jean, N. Geva, M. Welborn, T. Van Voorhis, V. Bulovic, M. G. Bawendi, M. A. Baldo, *Nat. Photonics* **2016**, *10*, 31.
[20] M. A. Filatov, S. Baluschev, K. Landfester, *Chem. Soc. Rev.* **2016**, *45*, 4668.
[21] Y. Zeng, J. P. Chen, T. J. Yu, G. Q. Yang, Y. Li, *Acs Energy Lett* **2017**, *2*, 357.
[22] A. Monguzzi, R. Tubino, S. Hoseinkhani, M. Campione, F. Meinardi, *PCCP* **2012**, *14*, 4322.
[23] R. P. Groff, P. Avakian, A. Suna, R. E. Merrifield, *Phys. Rev. Lett.* **1972**, *29*, 429.
[24] R. P. Groff, A. Suna, P. Avakian, R. E. Merrifield, *Phys. Rev. B* **1974**, *9*, 2655.
[25] J. Mezyk, R. Tubino, A. Monguzzi, A. Mech, F. Meinardi, *Phys. Rev. Lett.* **2009**, *102*.
[26] M. Oldenburg, A. Turshatov, D. Busko, S. Wollgarten, M. Adams, N. Baroni, A. Welle, E. Redel, C. Woll, B. S. Richards, I. A. Howard, *Adv. Mater.* **2016**, *28*, 8477.
[27] P. F. Duan, N. Yanai, Y. Kurashige, N. Kimizuka, *Angew. Chem., Int. Ed.* **2015**, *54*, 7544.
[28] K. Kamada, Y. Sakagami, T. Mizokuro, Y. Fujiwara, K. Kobayashi, K. Narushima, S. Hirata, M. Vacha, *Mater Horiz* **2017**, *4*, 83.
[29] S. M. A. Fateminia, Z. M. Wang, C. C. Goh, P. N. Manghnani, W. B. Wu, D. Mao, L. G. Ng, Z. J. Zhao, B. Z. Tang, B. Liu, *Adv. Mater.* **2017**, *29*.
[30] J. E. Kwon, S. Y. Park, *Adv. Mater.* **2011**, *23*, 3615.
[31] C. Zhang, Y. L. Yan, Y. S. Zhao, J. N. Yao, *Acc. Chem. Res.* **2014**, *47*, 3448.
[32] Y. Zhang, Q. Liao, X. G. Wang, J. N. Yao, H. B. Fu, *Angew. Chem., Int. Ed.* **2017**, *56*, 3616.
[33] Y. N. Hong, J. W. Y. Lam, B. Z. Tang, *Chem. Soc. Rev.* **2011**, *40*, 5361.
[34] J. Mei, N. L. C. Leung, R. T. K. Kwok, J. W. Y. Lam, B. Z. Tang, *Chem. Rev.* **2015**, *115*, 11718.
[35] S. A. Vinogradov, D. F. Wilson, *J Chem Soc Perk T 2* **1995**, 103.
[36] J. E. Rogers, K. A. Nguyen, D. C. Hufnagle, D. G. McLean, W. J. Su, K. M. Gossett, A. R. Burke, S. A. Vinogradov, R. Pachter, P. A. Fleitz, *J. Phys. Chem. A* **2003**, *107*, 11331.
[37] X. N. Cui, J. Z. Zhao, P. Yang, J. F. Sun, *Chem. Commun.* **2013**, *49*, 10221.
[38] J. T. He, B. Xu, F. P. Chen, H. J. Xia, K. P. Li, L. Ye, W. J. Tian, *J Phys Chem C* **2009**, *113*, 9892.
[39] Y. J. Dong, B. Xu, J. B. Zhang, H. G. Lu, S. P. Wen, F. P. Chen, J. T. He, B. Li, L. Ye, W. J. Tian, *Crystengcomm* **2012**, *14*, 6593.
[40] Y. J. Dong, B. Xu, J. B. Zhang, X. Tan, L. J. Wang, J. L. Chen, H. G. Lv, S. P. Wen, B. Li, L. Ye, B. Zou, W. J. Tian, *Angew. Chem., Int. Ed.* **2012**, *51*, 10782.
[41] L. L. Yan, Y. Zhang, B. Xu, W. J. Tian, *Nanoscale* **2016**, *8*, 2471.
[42] S. Baluschev, V. Yakutkin, T. Miteva, G. Wegner, T. Roberts, G. Nelles, A. Yasuda, S. Chernov, S. Aleshchenkov, A. Cheprakov, *New Journal of Physics* **2008**, *10*.
[43] A. Monguzzi, R. Tubino, F. Meinardi, *J. Phys. Chem. A* **2009**, *113*, 1171.
[44] A. Turshatov, D. Busko, S. Baluschev, T. Miteva, K. Landfester, *New Journal of Physics* **2011**, *13*.
[45] S. H. C. Askes, P. Brodie, G. Bruylants, S. Bonnet, *J. Phys. Chem. B* **2017**, *121*, 780.
[46] Z. Q. Xun, Y. Zeng, J. P. Chen, T. J. Yu, X. H. Zhang, G. Q. Yang, Y. Li, *Chem-Eur J* **2016**, *22*, 8654.
[47] A. Monguzzi, J. Mezyk, F. Scotognella, R. Tubino, F. Meinardi, *Phys. Rev. B* **2008**, *78*.
[48] J. C. deMello, H. F. Wittmann, R. H. Friend, *Adv. Mater.* **1997**, *9*, 230.
[49] Y. Y. Cheng, B. Fuckel, T. Khoury, R. G. C. R. Clady, M. J. Y. Tayebjee, N. J. Ekins-Daukes, M. J. Crossley, T. W. Schmidt, *J. Phys. Chem. Lett.* **2010**, *1*, 1795.
[50] A. Monguzzi, M. Mauri, M. Frigoli, J. Pedrini, R. Simonutti, C. Larpent, G. Vaccaro, M. Sassi, F. Meinardi, *J. Phys. Chem. Lett.* **2016**, *7*, 2779.

10.1002/cssc.201701389

WILEY-VCH

Entry for the Table of Contents

FULL PAPER

A light-harveting nanocrystal assembled by 9,10-distyrylanthracene and palladium(II) *meso*-tetraphenyltetrabenzoporphyrin in which red light is harvested and converted to green emission under incoherent excitation of low power density and the upconversion quantum yield of 0.29 ± 0.02% is obtained on account of the well-defined alignment of the molecules with aggregation-induced emission in the nanocrystals.

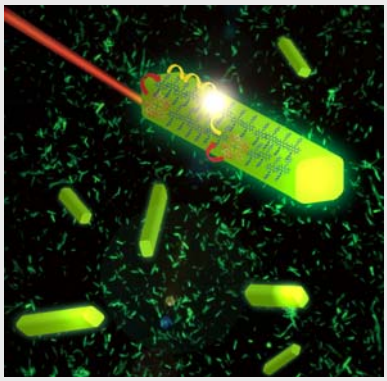

Li Li, Yi Zeng, Tianjun Yu, Jinping Chen, Guoqiang Yang, Yi Li**

Page No. – Page No.

Light-Harvesting Organic Nanocrystals Capable of Photon Upconversion